SIMULATION AND ANALYSIS OF A WWER-1000 REACTOR UNDER NORMAL AND TRANSIENT CONDITIONS

by

Ghonche BAGHBAN [1*], ***Mohsen SHAYESTEH*** [2], ***Majid BAHONAR*** [3], ***and Reza SAYAREH*** [1]

[1] Nuclear Science and Technology Research Institute, Atomic Energy Organization of Iran, Tehran, Iran
[2] Department of Physics, Imam Hussein University, Tehran, Iran
[3] Department of Nuclear Engineering, Science and Research Branch, Islamic Azad University, Tehran, Iran

Scientific paper
DOI: 10.2298/NTRP1603207B

An accurate analysis of the flow transient is very important in safety evaluation of a nuclear power plant. In this study, analysis of a WWER-1000 reactor is investigated. In order to perform this analysis, a model is developed to simulate the coupled kinetics and thermal-hydraulics of the reactor with a simple and accurate numerical algorithm. For thermal-hydraulic calculations, the four-equation drift-flux model is applied. Based on a multi-channel approach, core is divided into some regions. Each region has different characteristics as represented in a single fuel pin with its associated coolant channel. To obtain the core power distribution, point kinetic equations with different feedback effects are utilized. The appropriate initial and boundary conditions are considered and two situations of decreasing the coolant flow rate in a protected and unprotected core are analyzed. In addition to analysis of normal operation condition, a full range of thermal-hydraulic parameters is obtained for transients too. Finally, the data obtained from the model are compared with the calculations conducted using RELAP5/MOD3 code and Bushehr nuclear power plant data. It is shown that the model can provide accurate predictions for both steady-state and transient conditions.

Key words: RELAP5, drift-flux model, nuclear reactor, nuclear power plant, WWER-1000

INTRODUCTION

Recent researches in area of the nuclear power plants safety have signified the necessity of predicting the plant behavior during normal and transient conditions. In this respect, design basis accidents are one of the most important transients in the nuclear reactor safety. Instantaneous jamming of one primary coolant pump set shaft, which would result in rapid coolant flow decrease through the reactor core, is one of these accidents. For such events, the most unfavourable moment is the time when the accident starts, because in this case, simultaneous loss of coolant flow rate takes place in other loops of the reactor. It is expected that during this accident, the reactor protection systems mitigate the consequences. However, if this system does not work properly, the accident would cause unfavourable conditions in terms of core cooling.

Almost no analysis regarding uncontrolled loss of flow accident of a WWER-1000 reactor is reported in the available literature, while controlled loss of flow transient is addressed by some researches using thermal-hydraulic codes. In this respect, Grudev and Pavlova [1] performed the loss of flow transient at partial power conditions caused by the trip of one main coolant pump by a RELAP5/MOD3.2 model. Additionally, a loss of flow transient analysis was described for Kozloduy WWER-1000 nuclear power plant by ASTRA plant analyzer, while the attention was focused on the primary side behavior [2]. Moreover, Noori-Kalkhoran *et al*. [3], investigated the effects of decrease of coolant flow rate in a WWER-1000 core by coupling PARCS/COBRA-EN codes.

Different computational methods and models can be used to evaluate response of the systems in different situations. Nevertheless, finding the most appropriate technique for a special issue is a vital task. Totally, there are two main aspects in analyzing a transient: thermal-hydraulic and kinetics. Based on the thermal-hydraulic aspect, although there is no net void at the outlet of a PWR (here a WWER-1000 reactor) under normal operating conditions, boiling can occur throughout most of the core during some transients. The drift-flux model, which is developed by Zuber and Findlay [4], can be considered as one of the most commonly applied models for prediction of the two-phase flows [5]. This model is an approximate formulation in comparison with the more rigorous two-fluid formulation. Therefore, one can greatly reduce the difficulties,

* Corresponding author; e-mail: ghonche_baghban@yahoo.com

commonly encountered when employing a two-fluid model, such as mathematical complication and numerical instability caused by interfacial interaction terms [6]. However, because of its simplicity and applicability to a wide range of two-phase flow problems of practical interest, the drift-flux model is of considerable importance in two-phase flow studies [7].

Reactor kinetics, as another important aspect, can be analyzed by different models. This model provides the power behavior of the core during analyses. In fact, reactor protection system is responsible for controlling the system. If all the external control mechanisms of a reactor fail to respond to transients, the reactor behavior is determined solely by the reactivity feedbacks of the reactor. Therefore, our objective in this article is simulating the behavior of a WWER-1000 nuclear reactor during both protected and unprotected loss of flow transients. To take into account both of these situations, neutronic behavior of the reactor is calculated by using the point kinetics model.

Finally, in order to validate the obtained results, RELAP5 and final safety assessment report (FSAR) data of the Bushehr nuclear power plant (NPP), are used. It is shown that the system parameters such as reactor power, fuel and coolant temperatures, pressure and void fraction distribution can be accurately determined for this accident.

COMPUTATIONAL MODEL

Thermal-hydraulic model

Formulation of the flow field equations is based on a four-equation drift-flux model, in this paper. The most important assumption associated with the drift-flux model is that the dynamics of two phases can be expressed by the mixture-momentum equation with a kinematic constitutive equation specifying the relative motion between phases [8]. The one-dimensional unsteady forms of the balance equations are [9]

– mixture continuity equation

$$\frac{\partial \rho_m}{\partial t} \quad \frac{\partial(\bar{v}_m \rho_m)}{\partial z} \quad 0 \tag{1}$$

– gas continuity equation

$$\frac{\partial(\rho_g \alpha_g)}{\partial t} \quad \frac{\partial(\rho_g \alpha_g \bar{v}_m)}{\partial z} \quad \Gamma_g \quad \frac{\partial}{\partial z} \frac{\alpha_g \rho_g \rho_\ell}{\rho_m} \bar{V}_{gj} \tag{2}$$

– mixture momentum balance

$$\frac{\partial(\bar{v}_m \rho_m)}{\partial t} \quad \frac{\partial(\rho_m \bar{v}_m^{\,2})}{\partial z} \quad \frac{\partial p_m}{\partial z}$$
$$\frac{f_m \rho_m \bar{v}_m |\bar{v}_m|}{2D} \quad \rho_m g \quad \frac{\partial}{\partial z} \frac{\alpha_g \rho_g \rho_l}{(1 \quad \alpha_g)} \bar{V}_{gj}^2 \tag{3}$$

– mixture enthalpy-energy balance

$$\frac{\partial \rho_m h_m}{\partial t} \quad \frac{\partial(\rho_m h_m \bar{v}_m)}{\partial z}$$
$$\frac{q_w \zeta h}{A_z} \quad \frac{\partial}{\partial z} \frac{\alpha_g \rho_g \rho_l}{\rho_m} (h_g \quad h_l) \bar{V}_{gj}$$
$$\frac{\partial}{\partial z} \frac{\alpha_g \rho_g \rho_l}{\rho_m} (h_g \quad h_l) \bar{V}_{gj}$$
$$\frac{\partial p_m}{\partial t} \quad \bar{v}_m \quad \frac{\alpha_g (\rho_l \quad \rho_g)}{\rho_m} \bar{V}_{gj} \quad \frac{\partial p_m}{\partial z} \tag{4}$$

It should be mentioned that the physical values and parameters present in these relations are explained in the nomenclature section.

Constitutive models and materials

The equations listed in the previous section are not complemented without applying the appropriate constitutive equations. On the other hand, two most important parameters used in the area-averaged velocity in the mass continuity of the gas phase in drift-flux model are C_0 the distribution parameter and V_{gj}, the drift velocity, which represent the effects of void distribution, and the relative velocity between the phases, respectively. To obtain these parameters values, a throughout survey of the literature is performed and the most appropriate data are established in the present study [8, 10, 11]. The area-averaged velocity can be computed from [9]

$$\bar{V}_{gj} \quad \langle\langle v_g \rangle\rangle \quad \langle j \rangle \quad \langle\langle v_{gj} \rangle\rangle \quad (C_0 \quad 1)\langle j \rangle \tag{5}$$

Different heat-transfer and flow conditions are comprised in the presented model based on the considered situation. Heat transfer coefficient is applied to relate the heat transferred to fluid and the heat produced in the heat structure. Furthermore, flow resistance factor is applied to the momentum balance equation to estimate the friction pressure drop in a fluid flowing through a channel. Accordingly, the main corresponding correlations for both flow resistance factor and convection heat transfer coefficient are listed in tab. 1 for different flow regimes.

Finally, the vapour generation rate per unit volume is calculated [16]

$$\Gamma \quad \frac{q \ A_w}{V h_{fg}} \quad \frac{h_l \quad h_{cr}}{(h_{l,sat} \quad h_{cr})(1 \quad \varepsilon)} \tag{6}$$

Table 1. Flow regimes, heat transfer and flow resistance factor correlations

Regime	Heat transfer	Regime	Flow resistance
Single phase	Dittus-Boelter [12]	Single phase	Darcy factor Re < 2100 [15] Blasius 2100 < Re < 30000 [15] McAdams Re > 30000 [15]
Nucleate boiling	Chen correlation [13]	Two phase	EPRI correlation [14]
Critical heat flux	EPRI correlation [14]	–	–

where the quantity of ε, as the pumping factor, is defined by

$$\varepsilon \quad \frac{\rho_l (h_{l,sat} \quad h_l)}{\rho_g (h_{g,sat} \quad h_{l,sat})} \tag{7}$$

In the above model, the enthalpy corresponding to the bubble departure point, which is denoted as the critical enthalpy, is estimated from

$$h_{CR} \quad \begin{matrix} h_{l.sat} & \frac{StC_{pl}}{0.0065}, Pe \quad 70000 \\ h_{l.sat} & \frac{NuC_{pl}}{455}, Pe \quad 70000 \end{matrix} \tag{8}$$

It should be mentioned here that the thermo-physical properties of water and steam are calculated using the correlations from the international standard IAPWS-IF97 [17], while the properties of the heated structures materials (density, thermal conductivity and specific heat) are taken from temperature dependent correlations of MATPRO-11 [18].

Kinetic and decay heat model

Power generation in the reactor core consists of two parts: (1) the prompt power from fission (kinetic energy of fission fragments), (2) decay heat from short-lived and long-lived fission products. The time dependent behavior of the prompt power generation is calculated from a point-kinetics model with six groups of delayed neutrons

$$\frac{dq(t)}{dt} \quad \frac{R(t) \quad \beta}{\Lambda} q(t) \quad \sum_{i \quad 1}^{6} \lambda_i C_i(t) \tag{9}$$

$$\frac{dC_i(t)}{dt} \quad \frac{\beta_t}{\Lambda} q(t) \quad \lambda_i C_i(t) \quad i \quad 1,2,3,\ldots,6 \tag{10}$$

The appropriate initial conditions for eqs. (9) and (10) are

$$q(t \quad 0) \quad q_0 \quad \frac{\beta_i}{\Lambda\lambda_i} q_0 \quad C_i(t \quad 0) \tag{11}$$

The reactivity $R(t)$, consists of the external reactivity R_{ext}, describing the control rod motion, and the feedback reactivity R_{FB} describing the dependency of power on the fuel temperature, coolant temperature and coolant density

$$R(t) \quad R_{ext}(t) \quad R_{fuel}(t) \quad R_{coolant}(t) \quad R_{density}(t) \tag{12}$$

The external reactivity describes the reactivity effects of the control rods while the reactivity feedback contributions are calculated by the following functions

$$R_{fuel}(t) \quad \eta_{fuel}[\overline{T}_{fuel}(t) \quad \overline{T}_{ref,fuel}] \tag{13}$$

$$R_{coolant}(t) \quad \eta_{coolant}[\overline{T}_{coolant}(t) \quad \overline{T}_{ref,coolant}] \tag{14}$$

$$R_{density}(t) \quad \eta_{density}[\overline{\rho}_{coolant}(t) \quad \overline{\rho}_{ref,coolant}] \tag{15}$$

where T is the temperature and η – the reactivity coefficient. All the average values are calculated applying a volumetric averaging procedure. For unprotected core situation, the term R_{ext} in eq. (12) is omitted and only feedback effects play the role of controlling the reactor. Total produced power in the core is sum of the decay heat power and power obtained from the point kinetics equations. Decay heat is calculated based on the American National Standard for decay heat power in light water reactors, ANSI/ANS-5.1-1979.

Fuel heat transfer model

While balances equations describe thermal-hydraulic characteristics of the fluid flow, thermal behavior of the fuel rod is evaluated by one-dimensional heat conduction equation. Heat balance equation in cylindrical coordinate in unsteady form is written as [19]

$$\frac{1}{r}\frac{\partial}{\partial r} \quad rk\frac{\partial T}{\partial r} \quad q \quad \rho C_p \frac{\partial T}{\partial t} \tag{16}$$

where, the thermal source density, q**?**, depends on both position and time. The heat transfer model, which implies a wall-heating model and a heat transfer model from a heated wall to the fluid's bulk, computes the temperature distribution in the fuel at each axial segment. At the clad-coolant interface, the convection boundary condition is applied. Heat transfer between coolant and clad may take place by natural or forced convection, nucleate, transition or fully developed boiling, depending on the flow regime. The heat transfer coefficient is evaluated explicitly while the wall and fluid temperature are treated implicitly. Equation (17) represents this relation

$$q_{wall} \quad ht^n (T_{wall} \quad T_{coolant})^{n \quad 1} \tag{17}$$

It should be noted that here the fuel rods are in the forms of cylinders. The central holes in them, which are typical of a WWER-1000 reactor, are considered in this analysis. Therefore, the zero heat flow out of the inner surface of a fuel rod is used as another boundary condition in the fuel heat transfer model [19]

$$\left.\frac{\partial T}{\partial r}\right|_{r \quad r_{inner}} \quad 0 \tag{18}$$

where r is the radius of the rod and r_{inner} is the radius of the fuel rod hole.

NUMERICAL SOLUTION METHOD

The basic governing equations as well as constitutive relations construct our basic mathematical model. For coolant, based on the finite difference scheme, implicit approaches are employed to assure the numerical stability and computational efficiency. Using

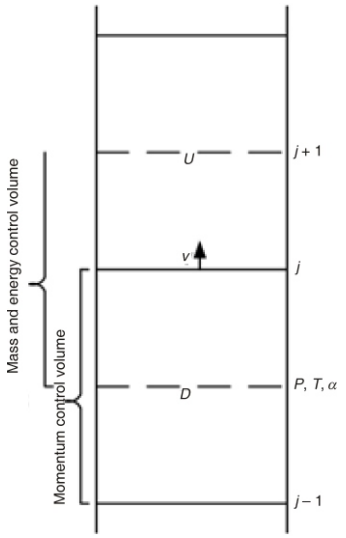

Figure 1. Nodalization scheme in the numerical modelling

a staggered arrangement of the variables based on fig. 1, balances equations of mass and energy are integrated over the mesh cells faces (from $j-1$ to j) while momentum equation is integrated between the centres of the mesh cells (from D to U). The state variables of pressure, temperature and void fraction are cell-centred while the flow variable is defined on junctions. Implicit Euler method is applied for the temporal derivative discretization ($n+1$ for new time and n for old time). On the cell faces, subscripts for the cell-centred quantities are U and D, while on the cell faces j increments are used (*e. g.* j, $j+1$, …). With these backgrounds, the difference equations are obtained as follows

– mixture continuity equation

$$\frac{1}{\Delta t}(\rho_m^{n+1} - \rho_m^n)_D - \frac{1}{\Delta z}[(\rho_m v_m)_j - (\rho_m v_m)_{j-1}]^{n+1} = 0 \tag{19}$$

– gas continuity equation

$$\frac{1}{\Delta t}(\rho_g^{n+1}\alpha^{n+1} - \rho_g^n\alpha^n)_D - \frac{1}{\Delta z}[(\rho_g \alpha v_m) - (\rho_g \alpha v_m)_{j-1}]^{n+1} - \Gamma_D^{n+1} - \frac{1}{\Delta z}\left[\frac{\alpha\rho_g\rho_l}{\rho_m}\bar{V}_{gj}\right]_j^{n+1} - \left[\frac{\alpha\rho_g\rho_l}{\rho_m}\bar{V}_{gj}\right]_{j-1} \tag{20}$$

– mixture momentum balance

$$\frac{1}{\Delta t}(\rho_m^{n+1} v_m^{n+1} - \rho_m^n v_m^n)_j - \frac{1}{\Delta z}[(\rho_m v_m^2)_U - (\rho_m v_m^2)_D]^{n+1} - \frac{1}{\Delta z}(P_U - P_D)^{n+1} - \frac{1}{\Delta z}\left[\frac{\alpha\rho_g\rho_l}{(1-\alpha)\rho_m}\bar{V}_{gj}^2\right]_U^{n+1} - \left[\frac{\alpha\rho_g\rho_l}{(1-\alpha)\rho_m}\bar{V}_{gj}^2\right]_D - \left[\frac{f_{TP}\rho_m v_m^2}{2D_e}\right]_j^{n+1} - \rho_{m,j}^{n+1} g \tag{21}$$

– mixture enthalpy-energy balance

$$\frac{1}{\Delta t}(\rho_m^{n+1} h_m^{n+1} - \rho_m^n h_m^n)_j - \frac{1}{\Delta z}[(\rho_m h_m v_m)_{j+1/2} - (\rho_m h_m v_m)_{j-1/2}]^{n+1} - \left[\frac{q P_h}{A_z}\right]^{n+1} - \frac{1}{\Delta z}\left[\frac{\alpha\rho_g\rho_l}{\rho_m}\right]_{j+1/2}^{n+1} - \left[\frac{\alpha\rho_g\rho_l}{\rho_m}\right]_{j-1/2} [(h_g - h_l)\bar{V}_{gj}]^{n+1} - \frac{1}{\Delta t}(P^{n+1} - P^n)_j - \frac{1}{\Delta z}\left[\frac{\alpha\rho_g\rho_l}{\rho_m}(h_g - h_l)\bar{V}_{gj}\right]_{j+1/2}^{n+1} - \left[\frac{\alpha\rho_g\rho_l}{\rho_m}(h_g - h_l)\bar{V}_{gj}\right]_{j-1/2} - v_m\left[\frac{\alpha(\rho_l - \rho_g)}{\rho_m}\bar{V}_{gj}\right]^{n+1} - \frac{1}{\Delta z}[(P)_{j+1/2} - (P)_{j-1/2}]^{n+1} \tag{22}$$

Additionally, to obtain the difference equation for heat conduction equation, the structures are divided into an arbitrary number of mesh cells. The temperatures are located at the edges of the mesh cells while the material properties are evaluated in the centres of the cells (fig. 2).

Finite difference approximation of the heat conduction equation is obtained by integrating eq. (16) between centres of two adjacent mesh cells, *i. e.* from $r_{i-1/2}$ to $r_{i+1/2}$. Since an implicit scheme is chosen for temporal discretization of eq. (16), the difference equation for the interior points in the fuel rod becomes

$$\frac{1}{2\Delta t}[r_i^2 - r_{i-1/2}^2)(\rho c_p)_{i-1/2}^{n+1} - (r_{i+1/2}^2 - r_i^2)(\rho c_p)_{i+1/2}^{n+1}](T^{n+1} - T^n)_i - \left[\frac{rk^n}{\Delta z}\right]_{i-1/2}[T_{i-1} - T_i]^{n+1} - \left[\frac{rk^n}{\Delta z}\right]_{i+1/2}[T_i - T_{i+1}]^{n+1} - \frac{1}{2}[(r_i^2 - r_{i-1/2}^2)(q)_{i-1/2}^{n+1} - (r_{i+1/2}^2 - r_i^2)(q)_{i+1/2}^{n+1}] \tag{23}$$

For numerical solution of the ordinary differential equations of the point kinetics model, a fourth-order Runge-Kutta method is used since these equations are in the form of ordinary stiff differential equations. Because of the stiffness associated with these equa-

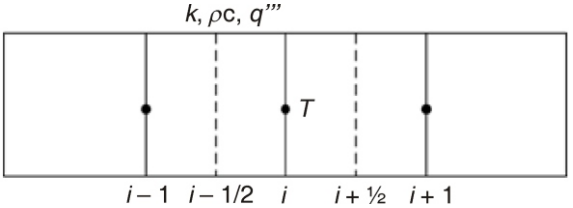

Figure 2. Fuel rod nodalization scheme in numerical modelling

tions, it is necessary to choose a numerical method with the capability to take into account this characteristic. Runge-Kutta method, applied in this paper, has fourth-order accuracy, which is higher than conventional first-order methods. However, this method does not have the complicity associated with higher order methods. Therefore, it is appropriate to be apply it in the presented model. Additionally, when trying to approximate the solution of a stiff differential equation, the step size considered in the discretization process should be small enough to prevent unstable solutions. In this study, time step size is chosen in such a way that an accurate solution can be attained. The maximum time step for the reactor kinetics advancement is one percent of the hydrodynamic time step. If this time step does not result to a stable solution, it is reduced until a stable solution is attained. This procedure is repeated in each time step.

The set of presented discretized coupled equations should be solved numerically. In fig. 3, a simple scheme of the calculation flow chart is shown. Flow chart has three main parts. In the fluid solution part, coolant parameters will be calculated using heat transfer rate from clad to coolant as input from fuel rod calculations. In the second and the third parts, fuel rod parameters and total power are calculated from heat conduction and point kinetics equations, respectively. Although, the main calculation procedure is not as simple as this scheme and each part itself includes some sub-sections. In fig. 4, a more elaborate scheme is shown for calculations.

Unknown main parameters of the pressure, temperature and void fraction distributions, are estimated. Meanwhile, each parameter is converged in a separate iteration loop. Furthermore, during each loop just a specific parameter is updated while all other main parameters are kept without change. This scheme continues for all the axial intervals. After acquiring the values of all the parameters, the calculations starts in the next time step using old values as initial values. Calculations stop when the transient ending time is reached. To make certain the calculations consistency, initial guesses of parameters in each time step is obtained from the previous time step values. This scheme makes iterations proceed fast and accurate.

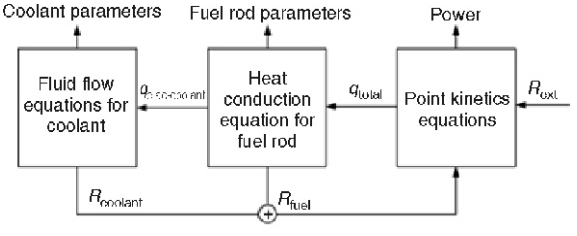

Figure 3. Relation between three different main solution parts

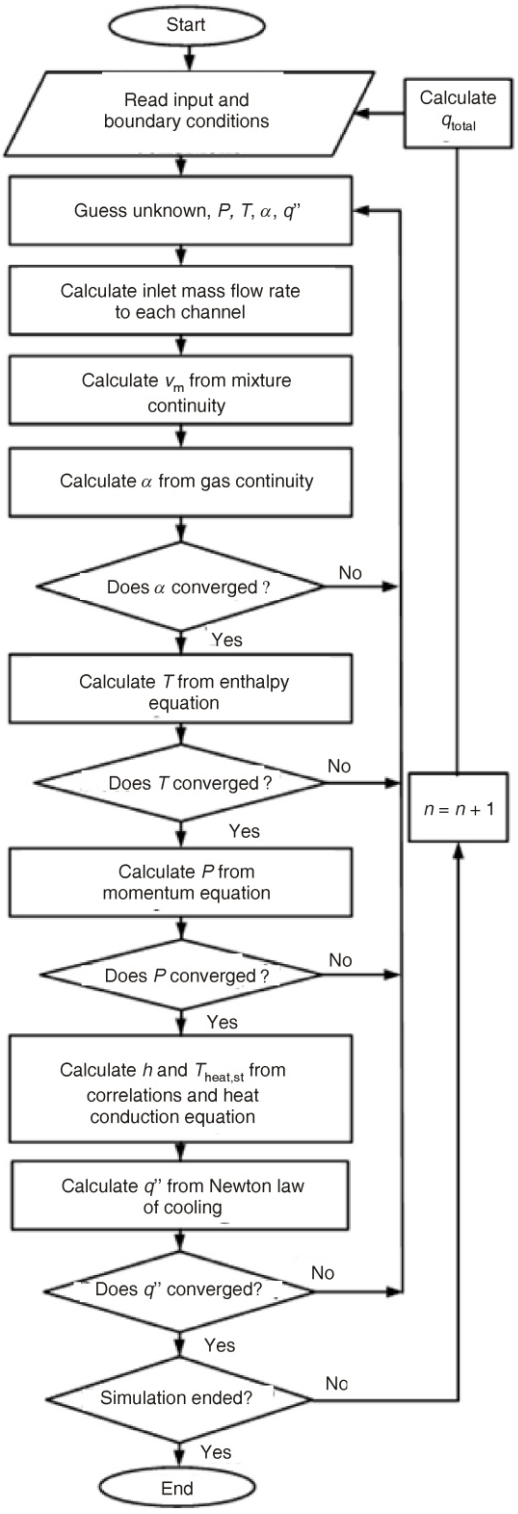

Figure 4. Flow chart of the solution

Fuel rod heat conduction equation is solved with a Gauss elimination method to obtain the temperature distribution of the fuel rod. The last part of the calculations is devoted to kinetics equations, which calculates the total core power. This power is then distributed between core fuel rods based on the power distribution factors.

Finally, in order to estimate the inlet flow distribution to each channel, it is assumed that the total flow

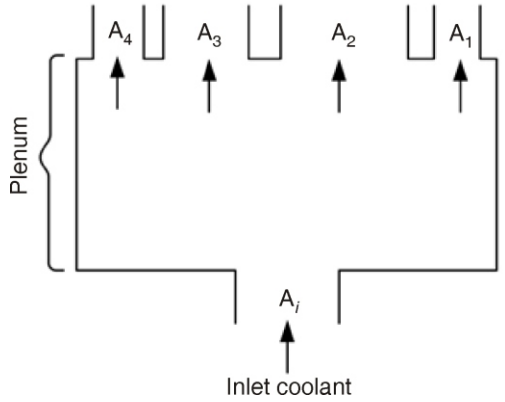

Figure 5. Coolant flow distribution in plenum A_1-A_4 – channel areas, A_i – inlet flow area

is first entered to lower plenum and then, it flows throughout the channels (fig. 5). Therefore, the flow through each channel is estimated using an iterative scheme, searching for the flow values that result in a unique pressure drop for all the channels inlets. However, because the cross-sectional area of the inlet flow, plenum and the channels are different, the dynamic head loss for abrupt flow area change is considered too. Since no heat is produced in the plenum, only continuity and momentum conservation equations are solved for the plenum model.

Initial and boundary conditions for fluid equations are inlet pressure, temperature, and total coolant mass flow rate. For kinetics equations external reactivity, as a function of time and initial reactor power, should be known.

RESULTS AND DISCUSSION

WWER-1000 reactor

WWER-1000 reactor is a vessel Russian-type pressurized water reactor with a four-loop primary system. Some of the main specifications of a WWER-1000 reactor (hear, Bushehr NPP) which are used in this article are presented in tab. 2. The fuel assemblies in the core are divided into three groups based on the power distribution. Radial power peaking factor for each fuel assembly, radial power peaking factor of fuel rods in each assembly and three constant sub-factors (axial power peaking factor, engineering safety factor and uncertainty coefficient) are assessed to estimate the power distribution in each group. Moreover, the individual corresponding channels of the fuel assemblies are lumped together to give an equivalent flow channel. Specifically, in order to perform the calculations in the present study, the core is divided into four parallel channels (three heated channels and an unheated bypass channel).

Channels are axially divided into 10 equal intervals while the fuel rods are divided into thirteen radial intervals with four intervals in clad and gap, and others in the fuel.

Table 2. Reactor specifications [20]

Reactor core operating conditions	Value
System pressure [MPa]	16.0
Reactor thermal power [MWt]	3120
Inlet coolant flow rate [m^3h^{-1}]	80000.0
Coolant temperature at the core inlet [K]	293
Maximum linear heat flux [Wcm^{-1}]	448
Fuel	
Hole diameter in the fuel pellet [mm]	1.5
Fuel pellet outside diameter [mm]	7.57
Cladding outside diameter [mm]	9.1
Fuel pellet material	UO_2
Cladding material	Zr-1% Nb alloy
Length of fuel rod [mm]	3530.0
Engineering safety factor	1.16
Uncertainty coefficient	1.04
Maximum radial peaking factor of hot rod	1.6
Fuel assembly flow area [mm^2]	25400.0
Fuel assembly wetted perimeter [mm]	9681.12
Fuel assembly heated perimeter [mm]	8919.0
Effective delay neutron fraction	0.007
Generation time [s^{-1}]	0.00002
Fuel temperature coefficient of reactivity [$°C^{-1}$]	–0.000018
Coolant temperature coefficient of reactivity [$°C^{-1}$]	–0.0001

Verification of the model

Since the full-scale experiments in area of the nuclear power plants safety are usually unpractical, results of the proposed model are assessed throughout comparing with the results from Bushehr NPP FSAR and the RELAP5/mod3 code. Analysis of the Bushehr NPP under condition of jamming of one reactor coolant pump is performed using code DINAMIKA-97, which is a Russian analysis code. Code DINAMIKA-97 is intended for analyzing the reactor plant conditions including normal operating conditions and anticipated operational occurrences [20]. On the other hand, The RELAP5/MOD3, which is a well-known system analysis code, uses non-equilibrium, two-fluid partially implicit general model for thermal-hydraulic analysis. The RELAP5/MOD3 code is developed for best-estimate transient simulation of the nuclear reactor systems during postulated accidents. More details of physical models in RELAP5/MOD3 can be found in the code manual reference book [21].

Steady-state results

Basic parameters of the system under steady-state conditions are summarized in tab. 3. From this table, it is obvious that the calculated values obtained by the model

agree well with the normal operation values reported in FSAR and those obtained by RELAP5/mod3 code. Steady-state results determine the initial conditions for transient calculations.

Transient calculations

Transient considered in this paper is instantaneous jamming of shaft of coolant pump, which would result to rapid coolant flow decrease through the reactor core. Two situations of loss of flow in protected and unprotected cores are considered. For protected loss of flow (with scram enabled), it is assumed that the reactor scram will occur within 1.9 s from the moment of transient initiation. With considering constant motion velocity of the control rods, their reactivity change versus time is assigned as the external reactivity to the kinetics equations. To perform the analyses, some initial and boundary conditions are extracted from FSAR data (tab. 2). Based on the flow coast down characteristics of the Bushehr NPP primary pumps, the coolant flow rate decays exponentially with time based on the data depicted in fig. 6, for both cases of transients. In addition, inlet core temperature and outlet pressure as other boundary conditions change during transient. These conditions are assigned as input to the problem (fig. 7).

With solving point kinetics equations, total power history of the core is obtained and depicted in fig. 8. It is evident from the figure that reactor power decreases rapidly with time after the control rods enter the core. Before this time, power essentially depends on the neutronic and thermal-hydraulic feedbacks. After scram, the power is determined totally based on the decay heat values. The results are in good agreement with results obtained from point kinetics model of the RELAP5 code and FSAR data.

With this power trend, figs. 9-11 show the core outlet temperature of the coolant as well as maximum fuel and clad outer surface temperatures. The temperatures start increasing from initiation of the transient and before scram occurs, because of loosing of core mass flow rate. However, after scram initiation these temperatures decrease due to a sudden decrease in reactor power and higher speed of decreasing power in comparison to the coolant flow rate.

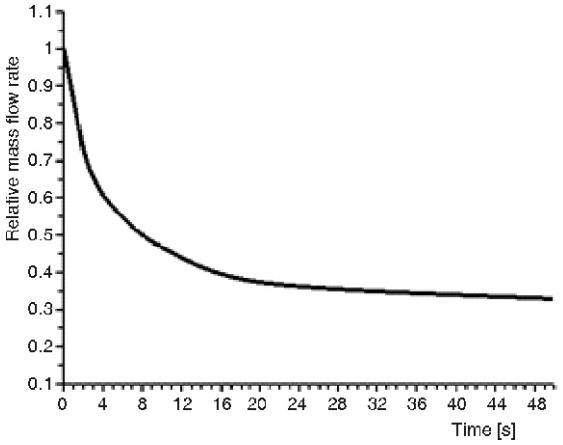

Figure 6. Relative core inlet mass flow rate

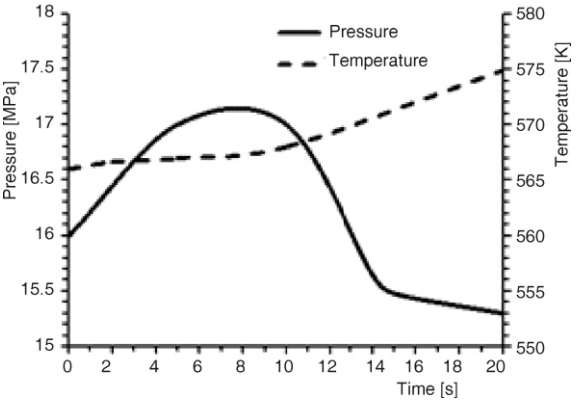

Figure 7. Relative reactor inlet temperature and outlet pressure

The inlet coolant mass flow rate to channels obtained from RELAP5 code and the flow division model of this study are compared in fig. 12.

In addition to aforementioned transient, a more severe condition of loss of flow transient without core protection is studied in this paper. For this transient, it is assumed that only feedbacks contribute to the solution. Reactivity introduced by feedback decreases power to some extent; however, this is not as effective as rod scram, in controlling the reactor. Other boundary and initial conditions are assumed same as before

Table 3. Calculated thermal-hydraulic parameters for the typical WWER-1000 reactor

Parameter	Obtained results	RELAP5 results	FSAR results [20]
Fuel inner surface maximum temperature [K]	2161.0	2120.0	2113.15
Clad outer surface maximum temperature [K]	623.9	623.7	<625.15
Mean coolant temperature at core exit [K]	597.9	598.2	598.15
Coolant maximum temperature at hot fuel channel [K]	610.0	609.0	n. a.
Channel 1 inlet velocity [ms^{-1}]	5.120	5.07	n. a.
Channel 2 inlet velocity [ms^{-1}]	5.133	5.10	n. a.
Channel 3 inlet velocity [ms^{-1}]	5.151	5.13	n. a.
Mean coolant density at hot fuel assembly outlet	629.3	633.1	n. a.
Mean coolant density at core exit [kgm^{-3}]	666.4	665.1	664.0

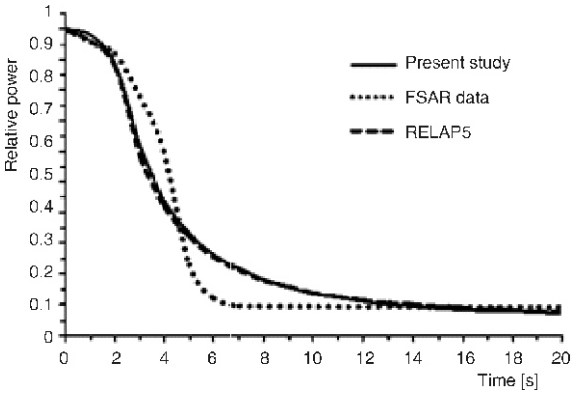

Figure 8. Total relative power of the reactor

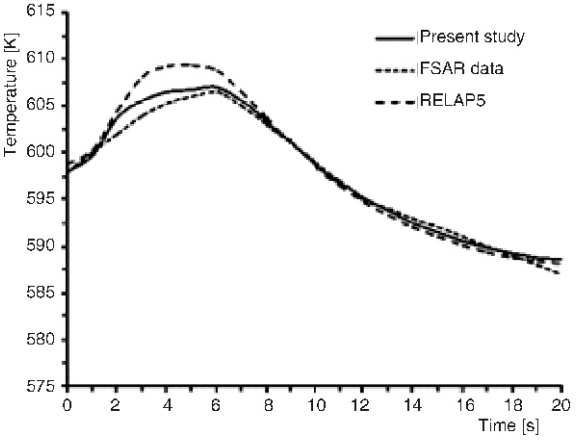

Figure 9. Core outlet coolant temperature for transient with scram

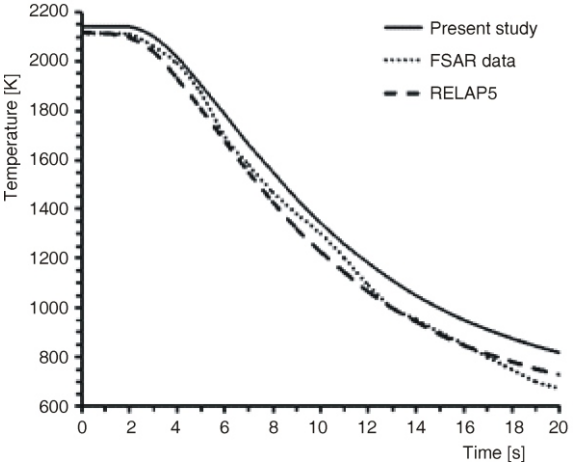

Figure 10. Maximum fuel temperature for transient with scram

in this condition. Total power change of the reactor is shown in fig. 13. Results for maximum coolant, fuel and clad temperatures, are depicted in figs. 14-16. Coolant and clad outside temperatures start increasing with decreasing of the coolant flow rate in this condition, while the fuel maximum temperature decreases since the rate of flow change is larger than the power decrease.

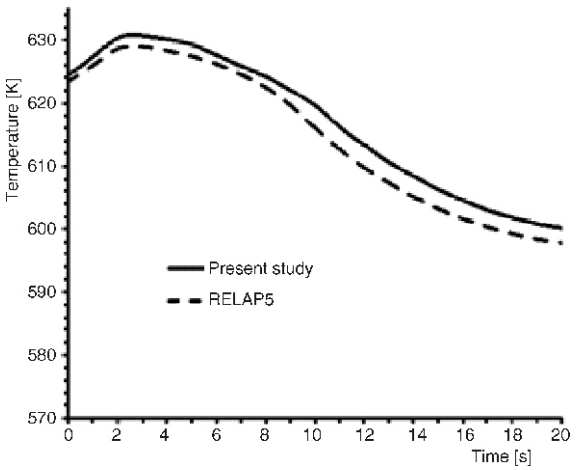

Figure 11. Maximum clad out surface temperature for transient with scram

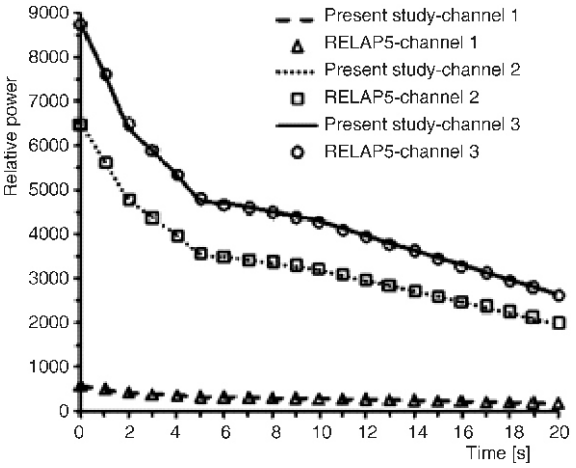

Figure 12. Inlet mass flow rate distribution in each channel

Moreover, it is possible for the coolant to become two-phase during this transient. Since the proposed model is capable of simulating a two-phase flow by taking advantage of drift-flux model, the void fraction is obtained. The results for the maximum value of the void fraction are shown in fig. 17. A good agreement between the results ascertains the ability of the presented two-phase simulation.

In order to show the compatibility between fuel and coolant parameters, void fraction distribution along the channels is shown in fig. 18 for time of 20s during this transient and the results are compared with the results obtained from RELAP5 code. Although there are some discrepancies between the results due to different solution methods, it is concluded that the model presented in this paper can estimate void fraction.

CONCLUSION

From the obtained results, it can be concluded that in the case of a flow transient with scram, the reactor remains in safe condition and all the temperatures are controlled from increasing beyond the safety is-

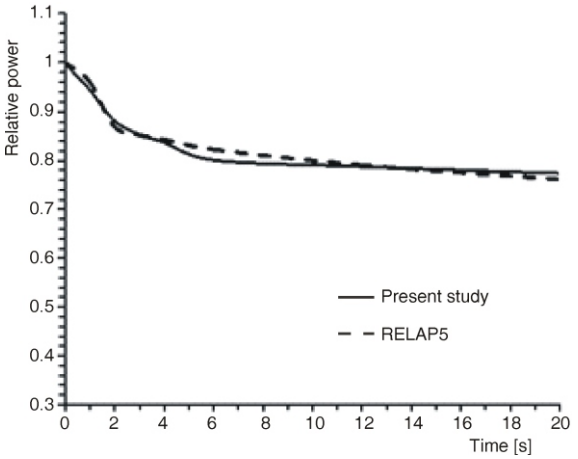

Figure 13. Total relative power of the reactor for transient without scram

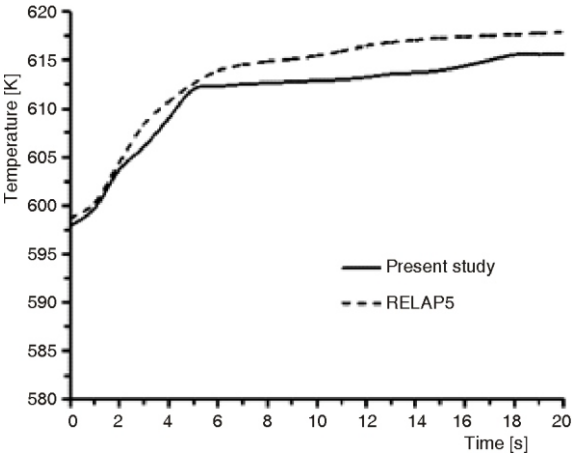

Figure 14. Core outlet temperature for transient without scram

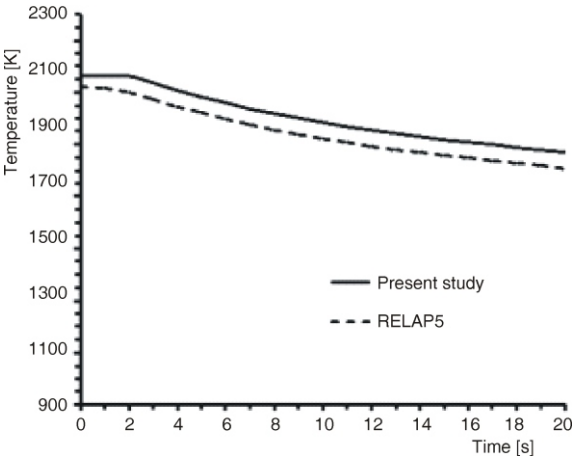

Figure 15. Maximum fuel temperature for transient without scram

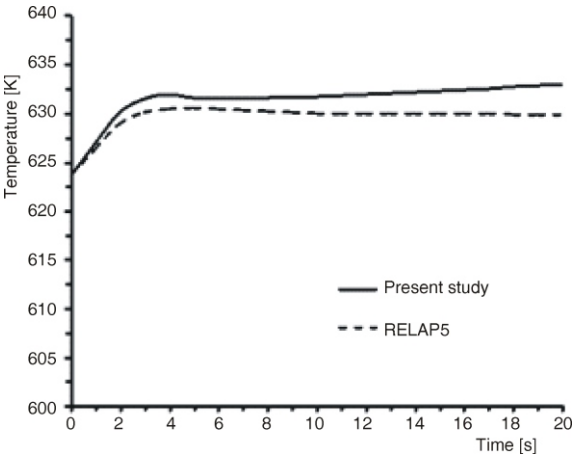

Figure 16. Maximum clad out surface temperature for transient without scram

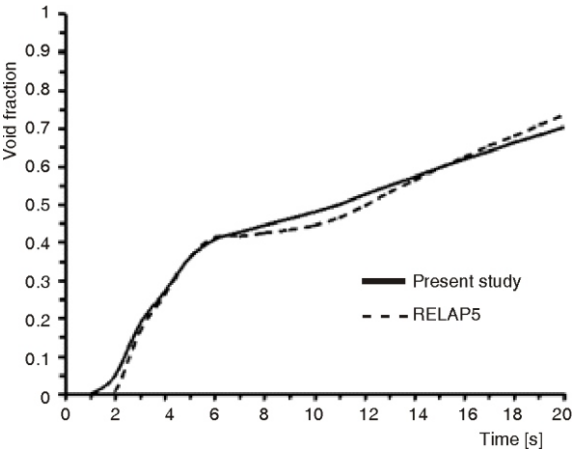

Figure 17. Maximum void fraction for transient without scram

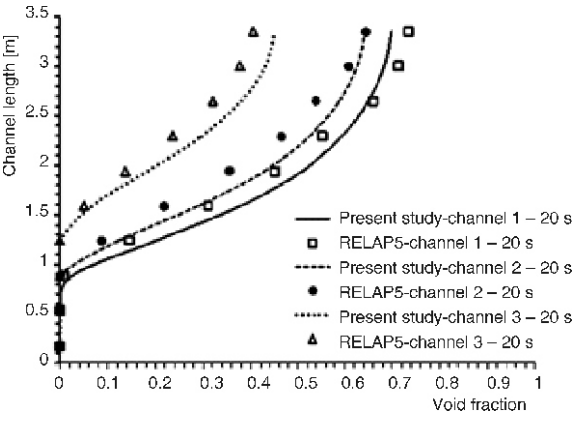

Figure 18. Void fraction distribution along the channels for simulation time of 20 s

sues; however, if scram cannot work well, only feedbacks' roles are taken into account, which are not as effective as the role of the control protection system. Finally, a good agreement between the computational results by two sets of the models (two-fluid in RELAP5 and drift-flux in the present study) is obtained, which proves the applicability and accuracy of the proposed model.

AUTHORS' CONTRIBUTIONS

The mathematical and numerical models were developed by G. Baghban under supervision of M. Shayesteh, M. Bahonar, and R. Sayareh. All the authors involved in discussing and analyzing the results. The data obtained from the RELAP5 were modelled by G. Baghban. The manuscript was written by G. Baghban and M. Bahonar and figures were prepared by G. Baghban. All the authors participated in preparation of the final version of the manuscript.

NOMENCLATURE

A – cross-sectional area, [m^2]
C – specific heat, [kJkg^{-1} °C]
C_i – neutron precursor concentration of group i, [kgm^{-3}]
D – diameter, [m]
f – friction coefficient
g – gravity acceleration, [ms^{-2}]
h – specific enthalpy, [kJkg^{-1}]
ht – heat transfer coefficient, [Wm^{-2}K^{-1}]
J – superficial velocity, [ms^{-1}]
k – thermal conductivity, [Wm^{-1}K^{-1}]
m – mass flow rate, [kgs^{-1}]
Nu – Nusselt number, ($=\beta l k^{-1}$)
P – pressure, [Pa]
Pr – Prandtl number, ($=C\mu k^{-1}$)
Pe – Peclet number, (=Re Pr)
q – heating power, [W]
Re – Reynolds number, ($=Dv\rho\mu^{-1}$)
R – reactivity, [$]
r – radius, [m]
St – Stanton number, (=Nu/Pe)
T – temperature, [K]
t – time, [s]
V – volume, [m^3]
v – velocity, [ms^{-1}]
z – height, [m]

Greek symbols

α – void fraction
β_i – delayed neutron fraction of group i
Γ – vapour generation rate per unit volume, [kgs^{-1}m^{-3}]
– difference
ε – pumping factor
Λ – neutron generation time, [s]
λ_i – decay constant of precursor group i, [s^{-1}]
μ – dynamic viscosity, [kgm^{-1}s^{-1}]
– perimeter, [m]
ρ – density, [kgm^{-3}]
τ – time constant, [s]

Subscripts and superscripts

″ – flux
‴ – per volume
cr – critical
fg – saturated liquid vapour difference
g – gas
g_j – superficial gas
h – heated
i – inner
l – liquid
m – mixture
0 – distribution
p – constant pressure
sat – saturated
w – wall
z – axial co-ordinate

Mathematical symbols

<> – area averaged quantity
<<>> – void fraction weighted area averaged quantity
– – mean value

REFERENCES

[1] Grudev, P., Pavlova, M., Simulation of Loss-of-Flow Transient in a VVER-1000 Nuclear Power Plant with RELAP5/MOD3.2, *Progress Nucl. Energy, 45* (2004), 1, pp. 1-10
[2] Amato, S., *et al*., Analysis of Loss of Flow Transients in the VVER-1000 Reactor Plant Analyzer, *Proccedings*, 2nd Regional Meeting in Nuclear Energy in Central Europe (Stritar, A., Jenčič, I.), Slovenia, September 11-14, 1995, pp. 482-489
[3] Noori-Kalkhoran, O., *et al*., Full Scope Thermal-Neutronic Analysis of LOFA in a WWER-1000 Reactor Core by Coupling PARCS v2.7 and COBRA-EN, *Progress Nucl. Energy, 74* (2014), 1, pp. 193-200
[4] Zuber, N., Findlay, J. A., Average Volumetric Concentration in Two-Phase Flow Systems, *ASME J. Heat Transfer, 87* (1965), 4, pp. 453-468
[5] Talebi, S., *et al*., A Numerical Technique for Analysis of Transient Two-Phase Flow in a Vertical Tube Using the Drift Flux Model, *Nucl. Eng. Des., 242* (2012), 1, pp. 316-322
[6] Gun, L.Y., Park, G. C., TAPINS: A Thermal-Hydraulic System Code for Transient Analysis of a Fully Passive Integral PWR, *Nucl. Eng. Technol., 45* (2013), 4, pp. 439-458
[7] Hibiki, T., Ishii, M., One-Dimensional Drift-Flux Model for Two-Phase Flow in a Large Diameter Pipe, *Int. J. Heat Mass Transfer, 46* (2003), 10, pp. 1773-1790
[8] Hibiki, T. M., Ishii, M., One-Dimensional Drift-Flux Model and Constitutive Equations for Relative Motion between Phases in Various Two-Phase Flow Regimes, *Int. J. Heat Mass Transfer, 46* (2003), 25, pp. 4935-4948
[9] Ishii, M., Hibiki, T., Thermo-Fluid Dynamics of Two-Phase Flow, Springer, New York, USA, 2006
[10] Coddington, P., Macian, R., A Study of the Performance of Void Fraction Correlations Used in the Context of Drift-Flux Two-Phase Flow Models, *Nucl. Eng. Des., 215* (2002), 3, pp. 199-216
[11] Schlegel, J., *et al*., Development of a Comprehensive Set of Drift-Flux Constitutive Models for Pipes of

Various Hydraulic Diameters, *Progress Nucl. Energy, 52* (2010), 7, pp. 666-677
[12] Dittus, F. W., Boelter, L. M. K., Heat Transfer in Automobile Radiators of the Tubular Type, University of California Press, Berkeley, Cal., USA, 1930
[13] Chen, J. C., A Correlation for Boiling Heat Transfer to Saturated Fluids in Convective Flow, *Ind. Eng. Chem. Process Des. Dev., 5* (1966), 3, pp. 322-329
[14] Basile, D., *et al*., COBRA-EN: an Upgraded Version of the COBRA-3C/MIT Code for Thermal Hydraulic Transient Analysis of Light Water Reactor Fuel Assemblies and Cores, ENELCRTN, Milano, Italy, 1999
[15] Todreas, N. E., Kazimi, M. S., Nuclear System-I, Thermal Hydraulic Fundamentals, Hemisphere Publishing Corporation, New York, USA, 1990
[16] Hari, H., Hassan, Y. A., Improvement of the Subcooled Boiling Model for Low-Pressure Conditions in Thermal-Hydraulic Codes, *Nucl. Eng. Des., 216* (2002), 1, pp. 139-152
[17] Wagner, W., Kruse, A., The Industrial Standard IAPWS-IF97 for the Thermodynamic Properties and Supplementary Equations for other Properties, Springer-Verlag, Heidelberg, Germany, 1998
[18] ***, IAEA, Thermo Physical Properties of Materials for Water-Cooled Reactors, International Atomic Energy Agency, Report IAEA-TECDOC-949, 1997
[19] El-Wakil, M. M., Nuclear Heat Transport, the American Nuclear Society, La Grange Park, Ill., USA, 1993
[20] ***, AEOI, Final Safety Analysis Report (FSAR) for Bushehr WWER-1000 Reactor Iran, Atomic Energy Organization of Iran, Tehran, Iran, 2007
[21] ***, The RELAP5 Code Development Team, RELAP5/MOD3 Code Manual, NUREG/CR-5535, INEL-95/0174, Idaho National Engineering Laboratory, Idaho Falls, USA, 1999

Received on June 2, 2015
Accepted on August 18, 2016

Гонч БАГХБАН, Мохсен ШАЈЕСТЕХ, Маџид БАХОНАР, Реза САЈАРЕХ

СИМУЛАЦИЈА И АНАЛИЗА НОРМАЛНИХ И ПРЕЛАЗНИХ СТАЊА РЕАКТОРА WWER-1000

Прецизна анализа тока прелазног стања веома је важна за оцену сигурности нуклеарне електране. У овом раду спроведена је анализа реактора WWER-1000, и у том циљу развијен је модел који симулира спрегнуту кинетику и термо-хидраулику реактора помоћу једноставног и прецизног нумеричког алгоритма. За термо-хидрауличне прорачуне примењен је модел четири једначине са дрифтованим флуксом. Језгро је издељено у неколико области у сагласности са вишеканалним приступом, при чему свака област приказујући једну горивну шипку са одговарајућим каналом за хлађење има сопствене карактеристике. Да се добије расподела снаге у језгру, коришћене су једначине тачкасте кинетике са различитим повратним спрегама. Разматрани су одговарајући иницијални и гранични услови и анализирана су два случаја слабљења јачине тока хладиоца у заштићеном и незаштићеном језгру. Поред анализе услова за нормалан рад, добијени су термо-хидраулични параметри за прелазна стања у пуном опсегу. На крају, коришћењем података о нуклеарној електрани Бушер, резултати добијени моделом упоређени су са прорачунима извршеним програмом RELAP5/MOD3. Показано је да модел обезбеђује прецизна предвиђања и стабилних и прелазних стања.

Кључне речи: RELAP5, модел дрифтованог флукса, нуклеарни реактор, нуклеарна електрана, WWER-1000